CONCRETE DRYING KINETICS: DEVELOPMENT OF AN ACCELERATED DRYING PROTOCOL IN FIRE TESTINGS

Takwa sayari, T Honorio, S Mohaine, F Robert, J.-L Adia, M Lion, P Gotteland, C Clergue, L Aloia, F Benboudjema

▶ **To cite this version:**

Takwa sayari, T Honorio, S Mohaine, F Robert, J.-L Adia, et al.. CONCRETE DRYING KINETICS: DEVELOPMENT OF AN ACCELERATED DRYING PROTOCOL IN FIRE TESTINGS. fib international congress 2022, Jun 2022, Oslo, Norway. ⟨hal-03712823⟩

HAL Id: hal-03712823

https://hal.science/hal-03712823v1

Submitted on 4 Jul 2022

HAL is a multi-disciplinary open access archive for the deposit and dissemination of scientific research documents, whether they are published or not. The documents may come from teaching and research institutions in France or abroad, or from public or private research centers.

L'archive ouverte pluridisciplinaire **HAL**, est destinée au dépôt et à la diffusion de documents scientifiques de niveau recherche, publiés ou non, émanant des établissements d'enseignement et de recherche français ou étrangers, des laboratoires publics ou privés.

HAL Authorization

CONCRETE DRYING KINETICS: DEVELOPMENT OF AN ACCELERATED DRYING PROTOCOL IN FIRE TESTINGS

T. Sayari[a,b], T. Honorio[a], S. Mohaine[b], F. Robert[b], J.-L. Adia[c], M. Lion[d], P. Gotteland[e], C. Clergue[f], L. d'Aloia[g], F. Benboudjema[a]

[a] Université Paris-Saclay, CentraleSupélec, ENS Paris-Saclay, CNRS, LMPS - Laboratoire de Mécanique Paris-Saclay, 91190, Gif-sur-Yvette, France

[b] Centre d'Essais au Feu du CERIB (Centre d'Etude et de Recherche de l'Industrie de Béton), Epernon, France

[c] EDF Lab. Les Renardières, Département MMC, Moret-sur-Loing, France

[d] EDF, Direction Industrielle, Département TEGG, Aix-en-Provence, France

[e] FNTP, Direction Technique Recherche, Paris, France

[f] EIFFAGE – Génie Civil, Département Innovation Représentation Matériaux (D.I.R.M.), Vélizy Villacoublay, France

[g] Centre d'Etudes des Tunnels (CETU), 69500 Bron, France

Abstract: This work proposes an accelerated drying protocol that allows reaching a hydric and mechanical state representative of normal service conditions while optimizing the storage time of the specimen before the fire resistance test. The temperature and relative humidity conditions are chosen in a range where microstructure changes are insignificant. An extensive experimental campaign on four concrete formulations is performed, including drying experiments (ambient and accelerated) and fire tests with different durations depending on the type of storage (normalized vs. accelerated drying). Then, the accelerated protocol is proposed based on the modeling of drying at moderate temperature. According to the predictive study, the target moisture content could be achieved under several drying conditions, showing that *ad hoc* solutions can be proposed. The reproducibility of the accelerated drying protocol is essential to ensure widespread application in research and industrial laboratories. This article focuses on the assessment of the water status.

Keywords: concrete drying kinetics, water content, concrete spalling fire, microstructure.

1. INTRODUCTION

The fire behavior of concrete is a critical aspect of civil engineering works since spalling, resulting from fire exposition, can lead to severe durability and safety problems. Fire characterization tests are therefore required to study and prevent spalling. The spalling of concrete is a complex phenomenon involving several mechanisms, such as water vapor pressure (liquid water can also be thermal pressurized), thermomechanical stresses, and deformation incompatibility between cement paste and aggregates [1]–[4]. Furthermore, it is strongly dependent on the hydric state and material permeability [5]. This means that if the concrete water content is high the day of the fire test and if it has low transfer properties, its resistance to spalling would be minor. The fire resistance test standard NF EN 1363-1 stipulates that at the testing time, the condition of the specimen should be representative of its normal service condition (mechanical strength and water content), considered to be obtained at equilibrium after storage in an ambient atmosphere. A conditioning period of at least three months is preconized. Drying processes play, therefore, a crucial role in the characterization of concrete susceptibility to spalling and should be studied carefully.

Concrete drying is a complex phenomenon involving several mechanisms, i.e., molecular diffusion, Knudsen diffusion, surface diffusion, and permeation. The hydric and hygric gradient between the material and its external environment generates the movement of: liquid water, water vapor, and dry air. Several research works focus on the description of the drying mechanisms [6]–[10] and show that concrete drying occurs in two main phases. The first phase is fast and lasts only a few hours to a few days. The second phase is much slower and evolves as a square root of time. This last phase is even slower in massive structures. So, the preconized conditioning period may underestimate the fire resistance due to higher spalling susceptibility associated with high water content. This shortcoming is

also reported by [11], who observed that a longer normalized conditioning time reduces the susceptibility of concrete to spalling.
This study aims at optimizing the fire test protocol by reducing the conditioning period via the definition of a hydric state representative of a structure with a few years of exploitation. The approach adopted is based on the combination of an experimental and numerical study of drying in concrete. The experimental campaign allows defining the material parameters (porosity, density, etc.), characterizing the drying kinetics (desorption isotherm test, mass loss monitoring, water content measurement, etc.), and validating the numerical predictions of the water profiles in concrete structures.

2. MATERIAL AND METHODS

2.1. Materials

To extend the reproducibility of the accelerated drying protocol and investigate its effectiveness on a wide range of concrete, four mix designs covering two prominent families of concrete were selected for this study. The table below shows the main characteristics of each mix design. The average compressive strength f_{cm} is measured at 28 days on 12 specimens per concrete. The porosity is measured at 28 days also according to the AFPC-AFREM recommendations. PERFDUB38 mix contains 8,4 % of silica fume and PERFDUB41mix contains 25 % of metakaolin.

Table 1 – The main characteristics of the studied concrete formulations.

Concrete formula	Source	f_{cm} [MPa]	Porosity [%] *
PERFDUB38	French national project PERFDUB [12]	86 ± 2,3	12,3 ± 0,2
PERFDUB41	French national project PERFDUB [12]	93 ± 3,3	11,7 ± 0,2
VERCORS	EDF [13]	45 ± 2,0	15,4 ± 0,3
CETU (containing polypropylene fibers)	CETU	44 ± 3,3	21,1 ± 0,9

* Corresponds to the standard deviation.

2.2. Concrete drying simulation

2.2.1. Drying at an ambient temperature

We briefly recall the nonlinear diffusion equation describing concrete drying. The formulation is based on the assumption of mass conservation and allows simulating the movement of water in its liquid and vapor forms in cementitious materials using the Darcy and Fick laws [14]. The liquid phase is assumed to be incompressible, so the density constant. The gaseous phase decomposes into dry air and water vapor. An isothermal temperature at 20 °C is considered [15], [16]. The Van Genuchten model is used to simulate the desorption isotherm [17]. Under these assumptions, the balance equation used to simulate the concrete drying at ambient temperature reads:

$$\rho_l \left[\Phi\left(1-\frac{\rho_v}{\rho_l}\right)\right]\frac{\partial S_l}{\partial t} = div\left[\frac{\partial p_c}{\partial S_l}\left(K_l\frac{\rho_l}{\mu_l} + D_v\frac{p_v}{\rho_l}\left(\frac{M_w}{RT}\right)^2\right) grad(S_l)\right] \quad (1)$$

where ρ_l liquid density, ρ_v vapor density, Φ porosity, p_c capillary pressure, S_l liquid water saturation degree, μ_l dynamic liquid viscosity, D_v diffusion coefficient, K_l apparent permeability, M_w molar density, R gas constant, T the temperature and t time.

Boundary conditions are Dirichlet-type ones. [10], [18], [19] show that this condition is sufficient to simulate drying in cementitious materials.

2.2.2. Drying at a moderate temperature

The choice of temperature is limited to moderate temperatures (up to 60 °C) to assume that no significant microstructural changes occur safely. For this study, the temperature is taken equal to 40 °C ± 2°C. The temperature effect on the material parameters (porosity, density, intrinsic permeability, etc.) is considered negligible [20]. We explicitly account for the temperature-dependence of the water viscosity [21] (cf. equation (2)), the saturation vapor pressure [22] (cf. equation (3)), the intrinsic diffusivity (cf. equation (5)) [23] and the desorption isotherm [24] (cf. equation (4)):

$$\mu_l = A_\mu 10^{\frac{B_\mu}{T - C_\mu}} \tag{2}$$

where T temperature, A_μ=2,414e^{-5} Pa, B_μ=247,8 K, and C_μ=140 K.

$$p_{vs} = p_{atm}.\, e^{\frac{40500}{R}\left(\frac{T-373}{373T}\right)} \tag{3}$$

where R=8,314 J mol^{-1} K^{-1} and p_{atm}= 101325 Pa.

$$S_l = \left[\left(\left(\frac{p_c}{a_{mu}(T)}\right)^{\frac{b_{mu}}{b_{mu}+1}} + 1\right)^{-\frac{1}{b_{mu}}}\right], \qquad a_{mu}(T) = a_{mu0} e^{\left(-\frac{T-T_0}{T_{kvgn}-T_0}\right)} \tag{4}$$

where T_0 reference temperature, a_{mu0}, b_{mu} and T_{kvgn} material parameters.

$$D_{v0} = 2{,}17.10^{-5}\frac{p_{atm}}{p_g}\left(\frac{T}{T_0}\right)^{1{,}88} \tag{5}$$

p_g gas pressure taken equal to p_{atm}.

Drying kinetics differ from one concrete to another depending on its porosity, pore size distribution, permeability, etc. Thierry [25] shows that ordinary concretes drying is driven mainly by the diffusion of water vapor, whereas in high-performance concrete concretes, the drying is driven primarily by the permeation of liquid water. Nonetheless, the temperature does not act the same way on the diffusion as on the permeation. The problem is even more complicated since the weight of each mechanism in the drying process is unknown. The acceleration factor obtained on VERCORS concrete with the adopted approach is compared to other methods in literature where an equivalent transfer coefficient is considered [26]–[28]. Figure 1 shows an acceleration factor of about 3.5 for diffusion and about 1.5 for permeation, going from 20°C to 40°C. To avoid this problem, an equivalent transfer coefficient will be used in the drying simulation, as shown in equation (6). The hydration and the wall effects are not considered in this model.

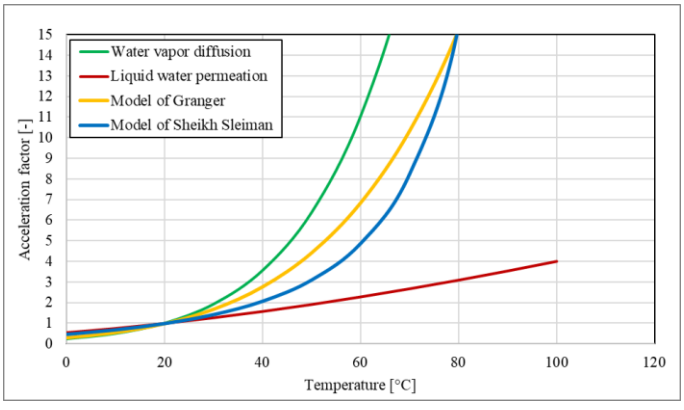

Figure 1 – Diffusion and permeation acceleration factor as a function of temperature. Comparison with factors obtained by other approaches in literature [26], [27].

$$\rho_l \left[\Phi\left(1 - \frac{\rho_v}{\rho_l}\right)\right]\frac{\partial S_l}{\partial t} = \mathrm{div}\left[\frac{\partial p_c}{\partial S_l}(K_{éq})\, grad(S_l)\right] \tag{6}$$

2.3. Experimental program

2.3.1. Drying kinetics characterization

The experimental characterization of the drying process consisted firstly of measurements of mass loss, porosity, and desorption isotherms for the numerical identification of the concrete transfer parameters. Mass loss experiments were conducted on cylinders Ø 11x10 cm to accelerate the equilibrium achievement while respecting the Representative Elementary Volume (generally superior or equal to 2.5 times the diameter of the largest aggregate). Thinner specimens (a few mm thick) were used to measure the desorption isotherm. Secondly, water content measures were carried out at different conditioning durations to validate the numerical prediction. The tests were launched in the two conditioning modes:

- 23 °C, 50 % RH which corresponds to the normalized conditioning, and
- 40 °C, 65 % RH which corresponds to the accelerated drying (defined numerically for each concrete).

The reference geometry corresponds to the geometry of the test bodies of the fire test, i.e., slabs of dimensions 1.7 x 1 x 0.3 m^3. for technical, operational reasons and to simplify the numerical study and the characterization of water profile evolution is carried out on cylinders Ø 15x30 cm which dry unidirectionally in height. This drying mode represents an element located in the middle of the slab (Figure 2).

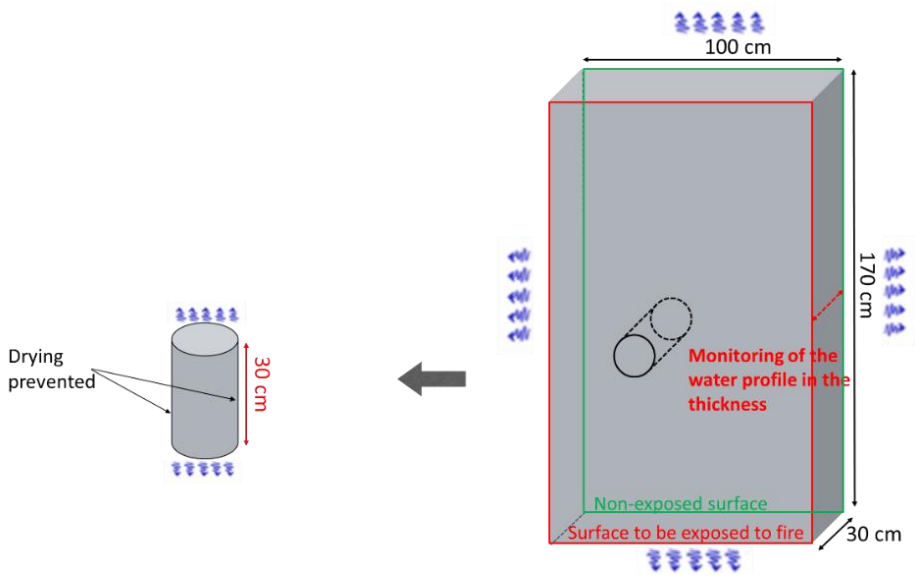

Figure 2 – The reference geometry and the drying configuration of the representative specimens.

2.3.2. Fire testing

Table 2 summarizes all the fire tests performed so far and provides the different parameters of the tests for each family of concrete (fire curve, loading, geometry of the specimens, and duration and conditioning mode). The tests carried out at three months of standardized conditioning correspond to the usual tests on concrete structures. An examination under the ISO 834 fire curve is conducted on PERFDUB concrete proof bodies subjected to the accelerated drying protocol. This accelerated drying is representative of a 3-month drying period under standard conditions according to the first approach of the numerical study. The objective of this first test is to evaluate the sensitivity to spalling in the drying modes (normalized vs. representative accelerated ones). One slab per concrete in an unloaded configuration is tested in each condition.

Table 2 – Assessment of the fire tests carried out to date

Concrete	Fire curves	Loading [MPa]	Specimens	Conditioning period	Conditioning mode
PERFDUB	ISO 834	0 and 4	Two slabs (1,7 x 1 x 0,3 m^3)	90 days	Normalized conditioning
	ISO 834	0	Two slabs (1,7 x 1 x 0,3 m^3)	15 days	Accelerated drying
Vercors and CETU	HCM	0 and 4	Two slabs (1,7 x 1 x 0,3 m^3)	90 days	Normalized conditioning

3. RESULTS AND DISCUSSION

3.1. Prediction of concrete drying under normalized conditioning

In the first part, the following figures illustrate the numerical results after identification of material parameters for VERCORS concrete compared to the experimental results. Figure 3 compares the theoretical/experimental results of the mass loss of a cylinder Ø 15x30 cm of VERCORS concrete drying unidirectionally. The results are consistent given the uncertainty associated with this measurement (± 0.1 % due to material variability).

Figure 4 shows the theoretical/experimental results of the average water content per 2.5 cm in VERCORS concrete. With only the first section, the theoretical and empirical results are very close considering the standard deviation on the experimental measurement. For the first slice, which corresponds to the skin area, the drying is underestimated, which may suggest the impact of wall effects (i.e., the impact of the formwork, microcracking, hydration evolution, etc.). The wall effects are not considered in the drying model at this study stage.

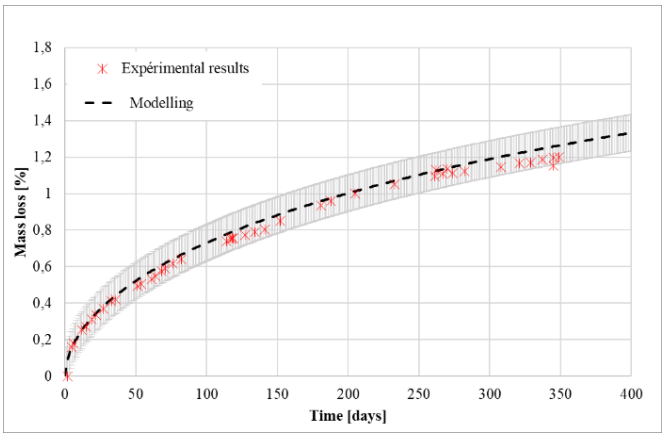

Figure 3 – Theoretical and experimental mass loss of a cylinder Ø 15x30 cm of VERCORS concrete drying uni-directionally.

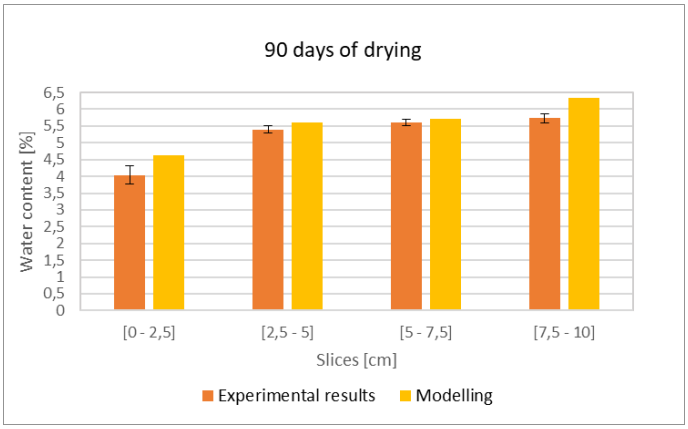

Figure 4 – Theoretical and experimental water content per cylinder Ø 15x30 cm slice of uni-directionally drying VERCORS concrete.

3.2. Development of an accelerated drying protocol

3.2.1. Numerical prediction and validation

Theoretically, to reach a similar water profile as a 23 °C, 50 % RH curing after 90 days, it is sufficient to cure for 15 days at 40 °C, 65 % RH with a 7-day conservation period in sealing condition before accelerated curing. This period is necessary to allow the hydration to progress. The allowed deviation is chosen to be equal to ± 0,4 % in absolute value for the water content. It is set to be equal to the maximum uncertainty value in the experimental measurements after a literature review. Experimental results are used in the numerical identification of drying parameters, and their uncertainty will propagate to the numerical results. In this case, it is not possible to set a more restrictive permissible deviation. The accelerated drying protocol is tested in the short term on PERFDUB38 concrete. The experimental results show good consistency between the moisture content measured in the two drying modes. The deviation is minimal and remains below the permissible deviation. This first test shows that it is possible to achieve a given moisture profile target by modifying the drying conditions and duration. This first short-term test of the accelerated protocol provides more confidence for the future and a test targeting a water profile at a few years of accelerated drying.

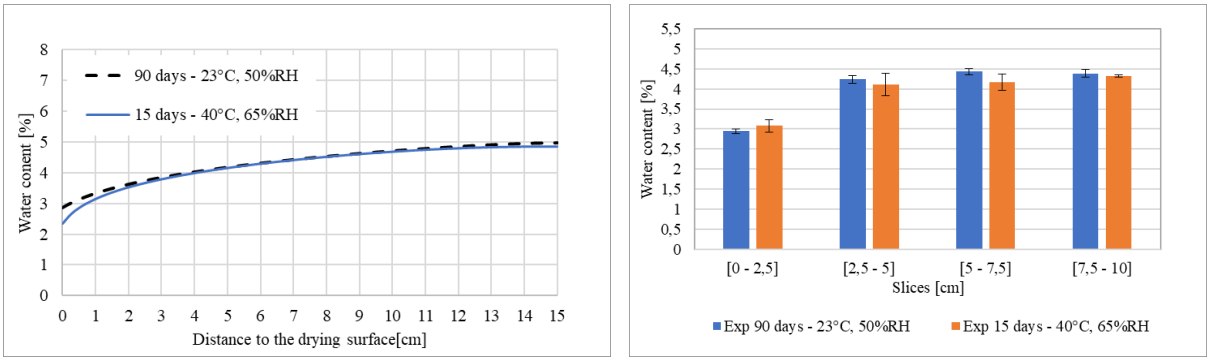

Figure 5 – Predicted water profile of a uni-directionally drying PERFDUB38 concrete after 90 days of normalized drying compared to the profile after 15 days of accelerated drying. On the right, the average water content per 2,5 cm from the drying surface to the core of Ø 15x30 cm cylinder.

3.2.1. Effect of accelerated drying on microstructure

Carbonation and microcracking are the two main possible microstructural changes that may occur because of the drying acceleration at moderate temperature.

Carbonation is maximal for a relative humidity range of about [40 % - 70 %]. The effect of temperature is more controversial in the literature [29]–[31], and the comparison of studies is not evident since the materials and test conditions are different. Papadakis and al. [32] have recently shown, through accelerated carbonation tests at temperatures ranging from 20 °C to 80°C, that carbonation increase linearly with temperature in concretes formulated with CEM I. However, the increase in the depth of carbonation is not significant. Therefore, the effect of the accelerated drying protocol (40 °C, 65 % RH) on the increase of the carbonation risk remains low. The evaluation of carbonation at 23 °C, 50 % RH and at 40 °C, 65 % RH confirms this hypothesis. The experiment consists of spraying Phenolphthalein on the Ø 11x10 cm cylinders having dried for 13 months uni-directionally. At 23 °C, 50 % RH, the carbonate thickness observed in PERFDUB concretes from 0 to 1 mm, from 0 to 3 mm in VERCORS concrete and from 2 to 5 mm in CETU concrete. At 40 °C, 65 % RH, the carbonate thickness observed in PERFDUB concretes varies from 0 to 2 mm. It varies in the same way in VERCORS concrete and from 2 to 3 mm in CETU concrete (Figure 6).

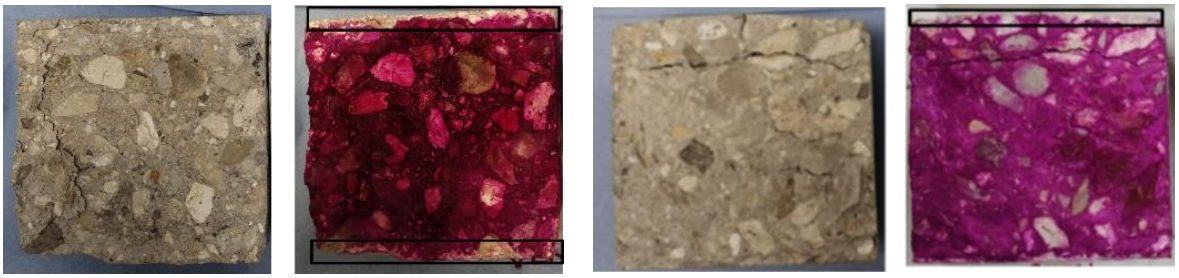

Figure 6 – Evaluation of carbonation by colored indicator (Phenolphthalein) in specimens of CETU concrete after unidirectional drying for 13 months at 23°C, 50% RH (left), and at 40 °C, 65 % RH (right).

Microcracking is observed with a Keyence optical microscope on Ø 11x10 cm cylinders dried at 40 °C, 65 % RH, and cylinders of the same geometry and size dried at 23 °C, 50 % RH. In both conditioning modes, the drying lasted 13 months and occurred in all directions. The maximum cracking rate and maximum openings are observed in the CETU concrete. Minor cracking is observed in VERCORS concrete. The PERFDUB concrete shows almost no cracking. This observation is valid for both drying modes. Comparing the cracking rate observed for the two drying modes in each concrete, the micro-cracking is almost identical for PERFDUB concretes, and more important in the case of drying at 23 °C for both VERCORS and CETU concretes. In this case, the effect of the deformations due to the thermal gradients passing from 23 °C to 40 °C might be negligible. The impact of the water gradient will be investigated to affirm whether drying at 23 °C, 50 % RH, induces more microcracking than drying at 40 °C, 65 % RH or not. For the moment, the result obtained is encouraging in the sense that the microcracking rate is not higher in the case of the accelerated drying.

Table 3 – Selection of microscopic cracking images (3300 x 2500 µm) on the PERFDUB38 and CETU concretes in the two drying modes (23 °C, 50 % RH) and (40 °C, 65 % RH).

Concrete	23 °C, 50 % RH	40 °C, 65 % RH
PERFDUB38		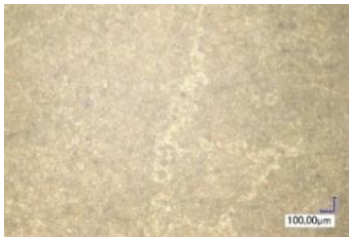
CETU		

3.3. Spalling sensibility: effect of the concrete conditioning

The effect of the conditioning mode on spalling due to fire has been tested on both PERFDUB mixes (§0). Table 4 shows the comparison of spalling sensibility, water content, and compressive strength between the normalised conditioning and the accelerated drying in the PERFDUB38 concrete mix. Results show good representativeness of the accelerated protocol compared to the normalized conditioning of 3 months. In the case of a drying time of 3 months, only the first centimeters of the specimen have dried, the core remains almost saturated. Therefore, for a water status representative of a short duration standardized drying (≤ 3 months), the 40 °C, 65 % RH accelerated drying protocol is validated. Furthermore, this accelerated drying protocol is also validated for a representative skin water status regardless of the drying duration. The same findings are observed on PERDUB41 concrete mix.

Table 4 – The impact of the storage conditions on the spalling susceptibility PERFDUB38 concrete mix.

Storage		90 days under 23 °C, 50 % RH	15 days under 40 °C, 65 % RH
f_{cm} [MPa]		91	88
Water content		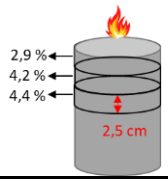	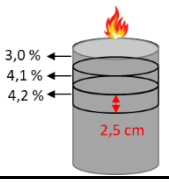
Spalling	Max depth [mm]	21	25
	Mean depth [mm]	12	12
	topography of the spalling		

4. CONCLUSION AND PERSPECTIVES

In this work, the experimental study allowed us to identify the concrete drying parameters and to validate the theoretical predictions. The drying prediction allowed us to evaluate the hydric profile evolution in the reference structure in short and long term and to define the target profile and then the optimal drying conditions to reach it in a few months only. The main conclusions are:

- The modeling of the drying phenomenon at different thermal and hydric solicitations shows that temperature plays an essential role in the acceleration of concrete drying. The relative humidity controls the water content on the surface of the test bodies but can delay in counterpart the drying if its value is high.
- According to the numerical results so far, drying during 15 days at 40°C, 65% RH after preservation in sealed condition for 7 days allows to reach the same water profile as for drying 90 days at 23 °C, 50% RH.

- Theoretically, several options of accelerated drying protocol are possible. A target water profile could be reached by different temperature and relative humidity combinations. In our study, the temperature is limited to 40°C in order to not to alter significantly the material microstructure.
- The first test of the accelerated drying protocol shows good consistency between theoretical predictions and experimental results of concrete water content. It also indicates that the accelerated drying did not modify the fire behavior.

Perspectives of this study include optimizing the numerical study by separating the two main drying mechanisms: and optimizing and refining the accelerated drying protocol by type of concrete. Also, we envision validating the accelerated drying protocol in the long term by assuming a target hydric state in a structure with a few years of operation. Applications of this study are broad and can go beyond fire behavior because of the strong dependence on the water profile of, for instance, delayed behavior and pathologies in concrete.

5. REFERENCES

[1] K. Hertz, 'Heat-induced explosion of dense concretes', *Technical University of Denmark, Institute of Building Design*, 1984.

[2] F. Robert, H. Colina, and G. Debicki, 'La durabilité des bétons face aux incendies', in *La durabilité des bétons*, Presses des Ponts et Chaussées., 2008.

[3] G. Choe, G. Kim, M. Yoon, E. Hwang, J. Nam, and N. Guncunski, 'Effect of moisture migration and water vapor pressure build-up with the heating rate on concrete spalling type', *Cement and Concrete Research*, vol. 116, pp. 1–10, Feb. 2019, doi: 10.1016/j.cemconres.2018.10.021.

[4] J.-C. Mindeguia, H. Carré, P. Pimienta, and C. L. Borderie, 'Experimental discussion on the mechanisms behind the fire spalling of concrete', Jun. 2014, Accessed: Nov. 08, 2019. [Online]. Available: https://hal-cstb.archives-ouvertes.fr/hal-01102429

[5] M. Maier, M. Zeiml, and R. Lackner, 'On the effect of pore-space properties and water saturation on explosive spalling of fire-loaded concrete', *Construction and Building Materials*, vol. 231, p. 117150, Jan. 2020, doi: 10.1016/j.conbuildmat.2019.117150.

[6] Y. Xi, Z. P. Bažant, L. Molina, and H. M. Jennings, 'Moisture diffusion in cementitious materials Moisture capacity and diffusivity', *Advanced Cement Based Materials*, vol. 1, no. 6, pp. 258–266, Nov. 1994, doi: 10.1016/1065-7355(94)90034-5.

[7] B. Bissonnette, P. Pierre, and M. Pigeon, 'Influence of key parameters on drying shrinkage of cementitious materials', 1999, doi: 10.1016/S0008-8846(99)00156-8.

[8] F. Benboudjema, 'Modelisation des deformations differees du beton sous sollicitations biaxiales. Application aux enceintes de confinement de batiments reacteurs des centrales nucleaires', Theses, Université de Marne la Vallée, 2002. Accessed: Nov. 12, 2019. [Online]. Available: https://tel.archives-ouvertes.fr/tel-00006945

[9] V. Baroghel-Bouny, 'Water Vapour Sorption Experiments on Hardened Cementitious Materials: Part I: Essential Tool for Analysis of Hygral Behaviour and its Relation to Pore Structure', *Cement and Concrete Research*, vol. 37, pp. 414–437, Mar. 2007, doi: 10.1016/j.cemconres.2006.11.019.

[10] J. Carette *et al.*, 'Identifying the mechanisms of concrete drying: An experimental-numerical approach', *Construction and Building Materials*, vol. 230, p. 117001, Jan. 2020, doi: 10.1016/j.conbuildmat.2019.117001.

[11] C. Lenglet, 'Evolution of spalling with time and age', *2nd international RILEM Workshop on concrete spalling due to fire exposure*, p. 6, 2011.

[12] 'Projet National PERFDUB', *PERFDUB*, 2019 2015. https://www.perfdub.fr/ (accessed Nov. 30, 2020).

[13] L. Charpin *et al.*, 'Ageing and air leakage assessment of a nuclear reactor containment mock-up: VERCORS 2nd benchmark', *Nuclear Engineering and Design*, vol. 377, p. 111136, Jun. 2021, doi: 10.1016/j.nucengdes.2021.111136.

[14] M. Mainguy, 'Modèles de diffusion non linéaire en milieux poreux. Applications a la dissolution et au séchage des matériaux cimentaires', Ph.D thesis, Ecole Nationale des Ponts et Chaussées, 1999. Accessed: Apr. 22, 2020. [Online]. Available: https://tel.archives-ouvertes.fr/tel-00869152

[15] M. Thiery, V. Baroghel-Bouny, N. Bourneton, G. Villain, and C. Stéfani, ‘Modélisation du séchage des bétons’, *Revue Européenne de Génie Civil*, vol. 11, no. 5, pp. 541–577, May 2007, doi: 10.1080/17747120.2007.9692945.
[16] M. Mainguy, O. Coussy, and V. Baroghel-Bouny, ‘Role of Air Pressure in Drying of Weakly Permeable Materials’, *Journal of Engineering Mechanics-asce - J ENG MECH-ASCE*, vol. 127, Jun. 2001, doi: 10.1061/(ASCE)0733-9399(2001)127:6(582).
[17] M. Th. van Genuchten, ‘A Closed-form Equation for Predicting the Hydraulic Conductivity of Unsaturated Soils’, *Soil Science Society of America Journal*, vol. 44, no. 5, pp. 892–898, 1980, doi: 10.2136/sssaj1980.03615995004400050002x.
[18] M. Bakhshi, B. Mobasher, and C. Soranakom, ‘Moisture loss characteristics of cement-based materials under early-age drying and shrinkage conditions’, *Construction and Building Materials*, vol. 30, pp. 413–425, May 2012, doi: 10.1016/j.conbuildmat.2011.11.015.
[19] Z. Zhang and U. M. Angst, ‘Effects of model boundary conditions on simulated drying kinetics and inversely determined liquid water permeability for cement-based materials’, *Drying Technology*, vol. 0, no. 0, pp. 1–18, Aug. 2021, doi: 10.1080/07373937.2021.1961800.
[20] CEN, ‘Eurocode 2: calcul des structures en béton - Partie 1-2: Règles générales - Calcul du comportement au feu. C. E. d. Normalisation.’ 2004.
[21] ‘Water - Density Viscosity Specific Weight | Engineering Reference and Online Tools’. https://www.engineersedge.com/physics/water__density_viscosity_specific_weight_13146.htm (accessed Jan. 27, 2022).
[22] B. Bary, M. V. G. de Morais, S. Poyet, and S. Durand, ‘Simulations of the thermo-hydro-mechanical behaviour of an annular reinforced concrete structure heated up to 200°C’, *Engineering Structures*, vol. 36, pp. 302–315, Mar. 2012, doi: 10.1016/j.engstruct.2011.12.007.
[23] D. De Vries and A. Kruger, ‘On the value of the diffusion coefficient of water vapour in air’, *In Proceedings of colloque Int. du CNRS*, vol. 160, p. 61u72, 1966.
[24] P. Chhun, ‘Modélisation du comportement thermo-hydro-chemo-mécanique des enceintes de confinement nucléaire en béton armé-précontraint’, Thèse, y, 2017. Accessed: Mar. 10, 2020. [Online]. Available: http://thesesups.ups-tlse.fr/3612/
[25] M. Thiery, ‘Modélisation de la carbonatation atmosphérique des matériaux cimentaires : prise en compte des effets cinétiques et des modifications microstructurales et hydriques’, These de doctorat, Marne-la-vallée, ENPC, 2005. Accessed: Jan. 12, 2022. [Online]. Available: http://www.theses.fr/2005ENPC0014
[26] L. Granger, ‘Comportement différé du béton dans les enceintes de centrales nucléaires : analyse et modélisation’, 1995. Accessed: Nov. 13, 2019. [Online]. Available: https://pastel.archives-ouvertes.fr/tel-00520675
[27] H. Cheikh Sleiman, M. Briffaut, S. Dal Pont, A. Tengattini, and B. Huet, ‘Influence of common simplifications on the drying of cement-based materials up to moderate temperatures’, *International Journal of Heat and Mass Transfer*, vol. 150, p. 119254, Apr. 2020, doi: 10.1016/j.ijheatmasstransfer.2019.119254.
[28] J.-L. D. Adia, H. Koala, J. Kinda, J. Sanahuja, and L. Charpin, ‘Concrete Drying Modelling in a Variable Temperature Environment’, in *Proceedings of the 3rd RILEM Spring Convention and Conference (RSCC 2020)*, Cham, 2022, pp. 47–58. doi: 10.1007/978-3-030-76465-4_5.
[29] T. Mori, K. Shiramayaka, K. Kamimura, and A. Yoda, ‘Carbonation of blast-furnace slag cement’, *Proceedings of the 26th annual meeting of cement association of Japan*, pp. 326–329, 1972.
[30] T. Uuomoto and Y. Takada, ‘Factors affecting concrete carbonation’, *Concrete library of JSCE (21)*, pp. 31–44, 1993.
[31] V. Papadakis, C. Vayenas, and M. Fardis, ‘Fundamental modeling and experimental investigation of concrete carbonation’, 1991, doi: 10.14359/1863.
[32] E. Drouet, S. Poyet, P. Le Bescop, J.-M. Torrenti, and X. Bourbon, ‘Carbonation of hardened cement pastes: Influence of temperature’, *Cement and Concrete Research*, vol. 115, pp. 445–459, Jan. 2019, doi: 10.1016/j.cemconres.2018.09.019.